Solid-State Electronics, 1977, Vol. 20, pp. 609–616. Pergamon Press. Printed in Great Britain

THE DOPANT DENSITY AND TEMPERATURE DEPENDENCE OF ELECTRON MOBILITY AND RESISTIVITY IN *n*-TYPE SILICON†

SHENG S. LI‡ and W. ROBERT THURBER

Semiconductor Processing Section, Electronic Technology Division, National Bureau of Standards, Washington, DC 20234, U.S.A.

(*Received* 18 *October* 1976)

Abstract—Traditional analysis of electron mobility in *n*-type silicon neglects the effect of electron–electron scattering in the mobility calculations. As a result, theory fails to conform with experiment when dopant density exceeds 2×10^{16} cm^{-3}. In this work, an improved theoretical model for computing mobility and resistivity as functions of dopant density and temperature has been developed for *n*-type silicon. The model has been applied to phosphorus-doped silicon for dopant densities from 10^{13} to 10^{19} cm^{-3}, and temperatures between 100 and 500 K. The mobility was calculated analytically by appropriately combining lattice, ionized impurity and neutral impurity scattering contributions. The effect of electron–electron scattering was incorporated empirically for dopant densities greater than 2×10^{16} cm^{-3}. Additionally, the anisotropic scattering effect was included in the mobility formulations. Resistivity measurements on seven phosphorus-doped silicon wafers with dopant densities from 1.2×10^{14} to 2.5×10^{18} cm^{-3} were carried out for temperatures from 100 to 500 K. Electron mobility at 300 K was deduced from resistivity and junction C-V measurements for dopant densities from 10^{14} to 10^{18} cm^{-3}. Agreement between theoretical calculations and experimental data for both electron mobility and resistivity of phosphorus-doped silicon was within ±7% in the range of dopant densities and temperatures studied.

NOTATION

- E electron energy
- E_C conduction band edge
- E_D donor energy level
- E_F Fermi energy
- E_N binding energy of neutral donors
- h Planck's constant, $=6.625\times10^{-34}$
- k Boltzmann's constant, $=1.38\times10^{-23}$
- m_0 free electron mass, $=9.1\times10^{-31}$
- m_n^* conductivity effective mass
- m_d^* density of states effective mass
- m_l^* longitudinal effective mass
- m_t^* transverse effective mass
- n electron density, cm^{-3}
- N_C effective density of conduction band states, cm^{-3}
- N_D total donor density, cm^{-3}
- N_D^+ ionized donor density, cm^{-3}
- N_I net ionized impurity density, cm^{-3}
- N_N neutral donor density, cm^{-3}
- q electronic charge, $=1.6\times10^{-19}$
- T absolute temperature, K
- ϵ_0 free space permittivity, $=8.854\times10^{-12}$
- ϵ_s permittivity of silicon, $=11.7\times\epsilon_0$
- ϵ_D donor ionization energy, $=(E_c-E_D)/q$ eV
- μ_L lattice scattering mobility, cm^2/V s
- μ_I ionized impurity scattering mobility, cm^2/V s
- μ_{LI} combined lattice and ionized impurity scattering mobility, cm^2/V s
- μ_N neutral impurity scattering mobility, cm^2/V s
- μ_n total electron mobility, cm^2/V s
- ρ electrical resistivity, Ω cm
- τ_I relaxation time of ionized impurity scattering.

Unless stated otherwise, all units are in MKS.

1. INTRODUCTION

Although a considerable amount of work has been published which deals with electrical properties and mobilities for silicon, it is evident that traditional analysis of electron mobility in *n*-type silicon fails to predict correctly the mobility values when dopant densities exceed 2×10^{16} cm^{-3}. The discrepancy may be attributed to the inadequacy of the existing theoretical models in the high dopant density range. For example, the effect of electron–electron scattering on both lattice and ionized impurity scattering mobilities has been neglected in the traditional analysis.

In this work, an improved theoretical model for computing electron mobility and resistivity as functions of dopant density and temperature for phosphorus-doped silicon is described. The calculations cover the range of dopant densities from 10^{13} to 10^{19} cm^{-3}, and temperatures between 100 and 500 K. A brief description of scattering theories and mobility formulations for *n*-type silicon is given in Section 2. Calculations of electron mobility and resistivity for phosphorus-doped silicon are presented in Section 3. Conclusions are given in Section 4.

2. SCATTERING MECHANISMS AND MOBILITY FORMULATION

In this section, a brief summary of the various scattering mechanisms that contribute to the total electron mobility in uncompensated *n*-type silicon is given.

†A more detailed version of this paper is to be published in NBS Special Publication 400-33. This work was conducted as a part of the Semiconductor Technology Program at NBS. Portions of this work were supported by the Defense Advanced Research Projects Agency (Order No. 2397, Program Code 5D10). Not subject to copyright. This work was carried out while the senior author (Li) was on a sabbatical leave from the University of Florida.

‡The permanent address is Department of Electrical Engineering, University of Florida, Gainesville, FL 32611, U.S.A.

Mobility formulation for each scattering process is discussed.

2.1 *Lattice scattering*

Lattice scattering mobility for *n*-type silicon has been calculated by Long[1], Norton *et al.*[2] and Rode[3], based on the general treatment of lattice scattering developed earlier by Herring and Vogt[4] for multivalley semiconductors. The calculations made by these investigators include contributions from both intravalley acoustical phonon scattering and intervalley optical phonon scattering. Additionally, the anisotropic scattering effect has also been included in these calculations. The theoretical calculations by Long and Norton agree well with their experimental data for lightly-doped *n*-type silicon in which lattice scattering is dominant. Consequently, it is pertinent for us to use the published lattice mobility data for the present mobility calculations. Values of lattice mobility calculated recently by Norton *et al.* (see Table IX of Ref. [2]) for phosphorus-doped silicon for $100 < T < 500$ K are listed in Table 1.

2.2 *Ionized impurity scattering*

For lightly-doped *n*-type silicon the main contribution to the electron mobility comes from lattice scattering. As the dopant density increases (or temperature decreases), the role of impurity scattering becomes more important. Theories for ionized impurity scattering in semiconductors have been developed by Brooks and Herring[5, 6], Dingle[7], Samoilovich *et al.*[8] and Luong and Shaw[9].

The Brooks–Herring formula is based on the important assumptions that the Born approximation applies, the relaxation time is a scalar, the energy surfaces are spherical, electron–electron interactions are negligible, and impurity cell effects can be ignored. The expression for the relaxation time derived from these assumptions, is[5, 6]

$$\tau_I = \frac{(2m_n^*)^{1/2}\epsilon_s^2 E^{3/2}}{\pi q^4 N_I G(b)} \times 10^{-6}, \tag{1}$$

where

$$G(b) = \ln(b+1) - b/(b+1), \tag{2}$$

$$b = \frac{24\pi m_n^* \epsilon_s (kT)^2}{q^2 h^2 n'} \times 10^{-6}, \tag{3}$$

and

$$n' = n \times (2 - n/N_D), \quad \text{for} \quad N_A = 0. \tag{4}$$

Equation (1) predicts that τ_I is proportional to $E^{3/2}$. The ionized impurity scattering mobility may be derived from eqn (1) with the result that[5]

$$\mu_{I(BH)} = \frac{2^{7/2}\epsilon_s^2 (kT)^{3/2}}{\pi^{3/2} q^3 m_n^{*1/2} N_I G(b)} \times 10^{-2}. \tag{5}$$

Equation (5) takes no explicit account of any anisotropy in the ion scattering. As a result, it usually overestimates the mobility values, particularly in the high dopant density range where impurity scattering is dominant.

The difficulty in using eqn (5) for computing ionized impurity scattering mobility lies in the choice of proper electron effective mass in eqns (3) and (5) when the energy band structure is nonspherical. For silicon, the anisotropic scattering effect comes from electron mass anisotropy (e.g. $m_t = 0.192m_0$, and $m_l = 0.98m_0$) due to the ellipsoidal conduction band structure. Long[9, 10] has made an extensive study of the validity of the Brooks–Herring formula for *n*-type silicon for dopant densities less than 10^{16} cm^{-3} and temperatures below 100 K. He concluded that if the electron effective mass in eqn (5) was used as an adjustable parameter, then good agreement between theory and experiment can be obtained. In the present study[32], we have also made a detailed comparison among the theoretical models developed by Brooks–Herring[5, 6], Conwell–Weisskopf[15] and Samoilovich *et al.*[8], and have found that the mobility values calculated from these models for *n*-type silicon are generally too large for $10^{13} < N_D < 10^{19}$ cm^{-3} and $100 < T < 500$ K. To correct this discrepancy, we have made use of the results of Long[5], and Norton *et al.*[2], and obtained a mobility expression, similar to that of eqn (5), for ionized impurity scattering:

$$\mu_I = 7.3 \times 10^{17}\, T^{3/2}/N_I G(b_l). \tag{6}$$

Here $G(b_l)$ is identical to eqn (2) with the exception that b is replaced by b_l, and $m_l^* = 0.98m_0$[18] is used in eqn (3) to obtain b_l. The numerical coefficient in eqn (6) was obtained directly from Ref. [10] for *n*-type silicon when the anisotropic scattering effect is included. The reader is referred to the original paper[10] for a complete description.

2.3 *Neutral impurity scattering*

Because of the analogy between a neutral donor atom and a hydrogen atom, the mobility for scattering by the neutral donors can be obtained by proper modification of the results for scattering of slow electrons by hydrogen atoms. Erginsoy first predicted a temperature-independent mobility given by[11]:

$$\mu_{NE} = \frac{2\pi^3 q^3 m_n^*}{5N_N \epsilon_s h^3} \times 10^{-2}. \tag{7}$$

Table 1. Lattice mobility of *n*-type silicon[2]

T (K)	100	130	160	200	250	300	350	400	500
$\mu_L\left(\frac{\text{cm}^2}{\text{V s}}\right)$	1.59×10^4	9.66×10^3	6.19×10^3	3.73×10^3	2.18×10^3	1.43×10^3	1.01×10^3	748	479

This equation fails to predict the temperature dependence of neutral impurity scattering mobility observed for n-type silicon at low temperatures[2]. Sclar[13] sought to improve eqn (7) by including the possibility of bound states in the electron-hydrogenic impurity scattering problem. He obtained the following expression for the neutral impurity scattering mobility[12]

$$\mu_N = 0.82\mu_{NE}\left[\frac{2}{3}\left(\frac{kT}{E_N}\right)^{1/2} + \frac{1}{3}\left(\frac{E_N}{kT}\right)^{1/2}\right], \tag{8}$$

where

$$E_N = 1.136 \times 10^{-19}(m_n^*/m_0)(\epsilon_0/\epsilon_s)^2 \tag{9}$$

and, μ_{NE} is given by eqn (7). Equation (8) predicts that μ_N varies as $T^{1/2}$ for kT above the binding energy, E_N. The experimental data given by Norton *et al.*[2] for n-type silicon show such a dependence up to 50 K. Our mobility and resistivity calculations using eqns (7) and (8) show that the latter produces a better fit with the experimental data than the former.

2.4 *Effect of electron–electron scattering*

The mobility formula given in eqn (6) neglects the effect of electron–electron (*e–e*) scattering on the ionized impurity scattering mobility. Although *e–e* scattering does not affect the current density directly since it cannot alter the total momentum, it tends to randomize the way in which this total momentum is distributed among electrons with different energy. When the scattering mechanism is such as to lead to a nonuniform distribution, *e–e* scattering gives rise to a net transfer of momentum from electrons which dissipate momentum less efficiently to those which dissipate momentum more efficiently, resulting in an over-all greater rate of momentum transfer and lower mobility.

On the basis of the above argument, it is obvious that the size of the effect of *e–e* scattering on the mobility is a function of the energy dependence of the relaxation time. Thus, for neutral impurity scattering where the relaxation time is independent of energy, the mobility is not affected by the *e–e* scattering. Ionized impurity scattering would be expected to be much more affected than lattice scattering since in the former case τ_I is proportional to $E^{3/2}$, while in the latter it is proportional to $E^{-1/2}$.

Luong and Shaw[13] have analyzed the effect of *e–e* scattering on the ionized impurity mobility using a single-particle-like approximation from the time-independent Hartree–Forck theory. They have shown that with the correction for *e–e* scattering, the Brooks–Herring formula is reduced by a factor which can be expressed in closed form as[13]

$$\mu_I'' = (1 - e^{-n/N_I}) \cdot \mu_I \tag{10}$$

where N_I is the ionized impurity density, n is the electron density, and μ_I is given by eqn (6). For uncompensated n-type silicon, the density of ionized donor impurities, N_I, is equal to the density of conduction electrons, n. Thus, eqn (10) reduces to

$$\mu_I'' = (1 - e^{-1})\mu_I = 0.632\mu_I \tag{11}$$

The factor in eqn (11) is in good agreement with a previous prediction[14] based on the Boltzmann theory. For n-type silicon, the effect of *e–e* scattering on the ionized impurity scattering becomes important for $N_D > 2 \times 10^{16}\,\text{cm}^{-3}$, as will be discussed later.

The effect of *e–e* scattering on the lattice mobility has also been discussed in several classical papers[5, 15, 16]. It can be shown[15, 16] that *e–e* scattering reduces the lattice scattering mobility by a maximum of 12%. Thus,

$$\mu_L'' = 0.88\mu_L. \tag{12}$$

3. RESULTS AND DISCUSSIONS

3.1 *Electron mobility vs donor density and temperature*

We now discuss the mobility calculations for n-type silicon in the range of dopant density from 10^{13} to $10^{19}\,\text{cm}^{-3}$ and temperature from 100 to 500 K. The combined mobility due to both lattice and ionized impurity scattering contributions can be calculated according to the mixed-scattering formula[15]

$$\mu_{LI} = \mu_L\left[1 + X^2\left\{Ci(X)\cos X + \sin X\left(Si(X) - \frac{\pi}{2}\right)\right\}\right] \tag{13}$$

where μ_L is the lattice mobility given in Table 1,

$$X^2 = 6\mu_L/\mu_I, \tag{13a}$$

and μ_I is given by eqn (6). $Ci(X)$ and $Si(X)$ are the cosine and sine integrals of X, respectively. Note that eqns (13) and (13a) are applicable for donor densities less than $2 \times 10^{16}\,\text{cm}^{-3}$ where the effect of *e–e* scattering is negligible. For dopant densities greater than $2 \times 10^{16}\,\text{cm}^{-3}$, the effect of *e–e* scattering is incorporated empirically in eqn (13) as follows:

(i) *High dopant density range* ($2 \times 10^{17} \leqslant N_D \leqslant 10^{19}\,cm^{-3}$). In this dopant density range, experimental evidence indicates that the full effect of *e–e* scattering should be taken into account in the mobility calculations, and eqn (13a) is replaced by

$$X''^2 = 6\mu_L''/\mu_I'', \tag{14}$$

where μ_L'' and μ_I'' are given by eqns (12) and (11) respectively.

(ii) *Intermediate dopant density range* ($2 \times 10^{16} \leqslant N_D \leqslant 2 \times 10^{17}\,cm^{-3}$). In this dopant density range, the effect of *e–e* scattering on both lattice and ionized impurity scattering mobilities is increased gradually with increasing dopant density. To obtain the best fit to the measured mobility at 300 K in this transition range, the mobility reduction factors, $R(N_D)$ and $S(N_D)$, for both μ_L and μ_I were derived empirically, assuming a linear dependence on the donor density. The results are given by:

$$\mu_L' = R(N_D)\mu_L, \tag{15}$$

where

$$R(N_D) = 1.013 - 6.63 \times 10^{-19} \times N_D \qquad (15a)$$

and

$$\mu_I' = S(N_D)\mu_I, \qquad (16)$$

where

$$S(N_D) = 1.04 - 2.04 \times 10^{-18} \times N_D. \qquad (16a)$$

The mobility ratio in eqn (13a) is now replaced by

$$X'^2 = 6\mu_L'/\mu_I'. \qquad (17)$$

Note that the mobility reduction factors, $R(N_D)$ and $S(N_D)$, in eqns (15a) and (16a), decrease linearly from 1 to 0.88 and 0.632, respectively, as the dopant density, N_D, increases from 2×10^{16} to 2×10^{17} cm^{-3} when full effect of e–e scattering is included. This allows a smooth change in mobility across the boundaries of the transition region.

Equations (12)–(17) allow the calculations of μ_{LI} for $10^{13} < N_D \leq 10^{19}$ cm^{-3} and $100 < T < 500$ K. When neutral impurity scattering is included, the total electron mobility may be computed from the expression

$$\mu_n = (\mu_{LI}^{-1} + \mu_N^{-1})^{-1} \qquad (18)$$

where μ_{LI} is given by eqn (12) and μ_N is the mobility due to neutral impurity scattering as given in eqn (8). A sum of the reciprocal mobilities for this case should yield a considerably better approximation than it does for the reciprocal sum of μ_L and μ_I because neutral impurity scattering, being independent of energy, does not affect any contributions from μ_L and μ_I.

The mobility formulas used in the present calculations are summarized in Table 2. As noted in this table the mobility calculations were carried out in three dopant density ranges. The criteria for establishing these three distinct dopant density ranges are based on our analysis of the electron mobility data versus dopant density at 300 K and the resistivity data for phosphorus-doped silicon taken at temperatures between 100 and 500 K. The mobility formulas in column (I) of Table 2 may be referred to as the traditional mobility formulations which neglect the effect of electron–electron scattering. The mobility calculations from these formulas for n-type silicon are in good agreement (within ±5%) with experimental data for dopant densities up to 2×10^{16} cm^{-3}, but for greater dopant densities the calculated mobility is larger than the measured mobility. By including the effect of e–e scattering in the mobility formulas shown in columns (II) and (III), we were able to bring into accord (within ±5%) the theoretical calculations and the experimental data at 300 K for dopant densities between 10^{13} and 10^{19} cm^{-3}. Figure 1 shows the electron mobility as a function of donor density computed using the appropriate formulas from Table 2 at 300 K, along with the experimental data for phosphorus-doped silicon. The solid dots are taken from the mobility data of Mousty *et al.*[24] and Baccarani

Table 2. Formulas for computing electron mobility in n-type silicon for $100 < T < 500$ K

(I) $10^{13} \leq N_D \leq 2 \times 10^{16}$ cm^{-3}	(II) $2 \times 10^{16} \leq N_D \leq 2 \times 10^{17}$ cm^{-3}	(III) $2 \times 10^{17} \leq N_D \leq 10^{19}$ cm^{-3}
(1) Lattice mobility[2]: μ_L Values of μ_L are listed in Table 1 ..... (1a)	(1) Lattice mobility: μ_L' $\mu_L' = R(N_D) \cdot \mu_L$ ..... (1b) where $R(N_D) = (1.013 - 6.62 \times 10^{-19} \times N_D)$	(1) Lattice mobility: μ_L'' $\mu_L'' = 0.88\mu_L$ ..... (1c)
(2) Ionized impurity mobility[10]: μ_I $\mu_I = 7.3 \times 10^{17} \times T^{3/2}/N_I G(b_i)$ ..... (2a) where $G(b_i) = \ln(b_i + 1) - b_i/(b_i + 1)$ $b_i = 1.52 \times 10^{15} \times T^2/n'$	(2) Ionized impurity mobility: μ_I' $\mu_I' = S(N_D) \cdot \mu_I$ ..... (2b) where $S(N_D) = (1.04 - 2.04 \times 10^{-18} \times N_D)$	(2) Ionized impurity mobility: μ_I'' $\mu_I'' = 0.632\mu_I$ ..... (2c)
(3) Mixed scattering formula for μ_{LI} [15]: $\mu_{LI} = \mu_L f(X)$ ..... (3a) where $f(X) = 1 + X^2(Ci(X)\cos X + \sin X(Si(X) - \pi/2))$ and $X^2 = 6\mu_L/\mu_I$	(3) Mixed scattering formula for μ_{LI}' $\mu_{LI}' = \mu_L' f(X')$ ..... (3b) where $X'^2 = 6\mu_L'/\mu_I'$	(3) Mixed scattering formula for μ_{LI}'' $\mu_{LI}'' = \mu_L'' f(X'')$ ..... (3c) where $X''^2 = 6\mu_L''/\mu_I''$
(4) Neutral impurity mobility[12]: μ_N $\mu_N = (3 \times 10^{20}/N_N) \cdot (0.1495 T^{1/2} + 1.482/T^{1/2})$ ..... (4a)	(4) Neutral impurity mobility: μ_N same as (4a) ..... (4b)	(4) Neutral impurity mobility: μ_N same as (4a) ..... (4c)
(5) Total electron mobility: μ_n $\mu_n = (1/\mu_{LI} + 1/\mu_N)^{-1}$ ..... (5a)	(5) Total electron mobility: μ_n $\mu_n = (1/\mu_{LI}' + 1/\mu_N)^{-1}$ ..... (5b)	(5) Total electron mobility: μ_n $\mu_n = (1/\mu_{LI}'' + 1/\mu_N)^{-1}$ ..... (5c)

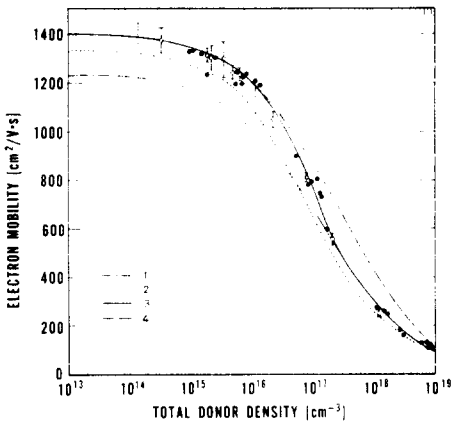

Fig. 1. Electron mobility vs total donor density for n-type silicon at 300 K. Curve 1 is the theoretical calculation with e–e scattering included for $10^{13} < N_D < 10^{19}\,\mathrm{cm}^{-3}$, curve 2 is the Irvin curve calculated from the Caughey and Thomas empirical formula[30], curve 3 is the exact theoretical calculation using mobility formulas in Table 2, curve 4 is the theoretical calculation with e–e scattering neglected. Open circles are from Buehler *et al.*[27], and solid dots are from Mousty *et al.*[24] for phosphorus-doped silicon.

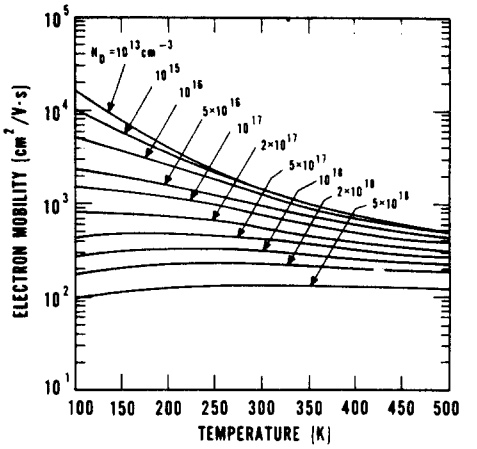

Fig. 2. Electron mobility of n-type silicon vs temperature for dopant densities from 10^{13} to $5\times10^{18}\,\mathrm{cm}^{-3}$.

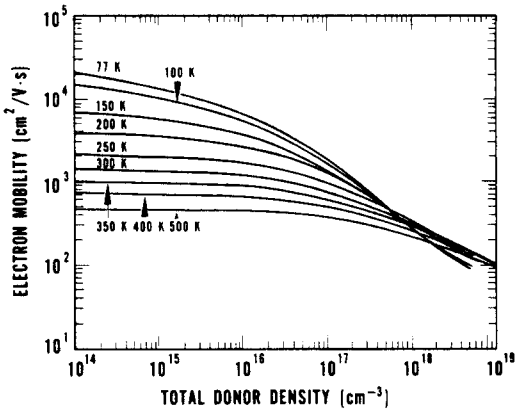

Fig. 3. Electron mobility of n-type silicon vs total donor density with temperature as a parameter ($77 < T < 500$ K).

and Ostoja[28], corrected to 300 K. The open circles are data obtained by Buehler *et al.*[27, 29] on processed phosphorus-doped silicon slices; a planar four-probe structure[27] was used for resistivity measurements and a diffused diode near to the four-probe test structure was used for junction C–V measurements of donor density[29]. The theoretical calculations, using formulas in Table 2 (curve 3), are within ±5% of the experimental data for dopant densities from 10^{14} to 10^{19} cm. For comparison, the Irvin mobility curve which was calculated from the Caughey and Thomas[30] empirical formula for n-type silicon is also shown by a dashed line (curve 2) in Fig. 1.

To illustrate the important effect of e–e scattering, we have also shown in Fig. 1 the theoretical calculations of electron mobility as a function of dopant density with (curve 1) and without (curve 4) inclusion of e–e scattering for the entire range of dopant densities from 10^{13} to $10^{19}\,\mathrm{cm}^{-3}$. It is clearly demonstrated that the mobility values predicted when e–e scattering is included (curve 1) are smaller than the measured mobility for $N_D \leqslant 2\times10^{17}\,\mathrm{cm}^{-3}$. On the other hand, the mobility values predicted when e–e scattering is neglected (curve 4) are larger than the measured mobility for $N_D > 2\times10^{16}\,\mathrm{cm}^{-3}$. Thus, a transition region (i.e. $2\times10^{16} \leqslant N_D \leqslant 2\times10^{17}\,\mathrm{cm}^{-3}$) exists in which the effect of e–e scattering increases gradually with increasing dopant density.

The mobility formulas in Table 2 were also used to compute the electron mobility as a function of dopant density for temperatures between 100 and 500 K. The results are displayed in Figs. 2 and 3.

3.2 *Calculation of the ionized donor density*

In this section, formulations are given for computing the ionized donor density (or electron density) as a function of the total donor density in uncompensated n-type silicon. In order to compute the electron mobility and resistivity, it is necessary to know the amounts of ionized and neutral impurity atoms so that their scattering contributions can be calculated.

The ionized donor densities for n-type silicon were computed by solving the charge balance equation for the Fermi energy by an iteration procedure. Since the minority carrier density (i.e. hole density in n-type silicon) is negligibly small for this case, the charge balance equation is simply

$$n \simeq N_D^+ \tag{19}$$

where[17]

$$N_D^+ = \frac{N_D}{1 + 2\exp\left[(E_F - E_C + E_D)/kT\right]}, \tag{20}$$

and the electron density, n, is given by[17]

$$n = N_C/[\exp(E_C - E_F)/kT + 0.27], \quad \text{for} \quad E_F < 1.3kT \tag{21}$$

where

$$N_C = 2\left[\frac{2\pi m_d^* kT}{h^2}\right]^{3/2}$$

is the effective density of conduction band states

($N_C = 3.22 \times 10^{19}\,cm^{-3}$ for n-type silicon at 300 K). The temperature dependence of the density of states effective mass was taken into account in accordance with the results of Barber[18].

Experimental evidence exists which shows that the donor ionization energy, ϵ_D, is not constant, but decreases with increasing dopant density. Hall coefficient measurements by Pearson and Bardeen[19] and more recently by Penin *et al.*[20] in heavily-doped silicon from 4 to 300 K show no evidence of an ionization energy at impurity densities greater than $3 \times 10^{18}\,cm^{-3}$. For n-type silicon doped with phosphorus impurities, the dependence of donor ionization energy on the dopant density is[15]

$$\epsilon_D = \epsilon_D(0) - \alpha N_D^{1/3} \tag{22}$$

where $\epsilon_D(0) = 0.045$ eV is the ionization energy of the phosphorus donor; with $\alpha = 3.1 \times 10^{-8}$ eV/cm, eqn (22) gives a zero ionization energy at $N_D = 3 \times 10^{18}\,cm^{-3}$. For $N_D > 3 \times 10^{18}\,cm^{-3}$, the electron density and the ionized donor density are computed from eqns (19) and (20), assuming $\epsilon_D = 0$. This result is also applied to the calculation of electron mobility for $N_D > 3 \times 10^{18}\,cm^{-3}$. The validity of the theoretical calculations for $N_D > 3 \times 10^{18}\,cm^{-3}$ needs further study and is beyond the scope of the present work.

In Fig. 4, the theoretical curves are shown for the percent ionization of phosphorus atoms versus total phosphorus density for temperatures between 100 and 500 K. The electron density was obtained from eqn (19), which is a valid approximation for the uncompensated case.

3.3 *Resistivity vs donor density and temperature*

Measurements of resistivity in silicon have been reported by previous investigators[23–35]. Irvin[23] first showed complete resistivity versus dopant density curves for both n- and p-type silicon at 300 K, using mostly previously published data. Recently Mousty *et al.*[24] reported the resistivity versus phosphorus density in n-type silicon. The electrical properties of heavily doped silicon were also reported by Chapman *et al.*[26]. Most of these efforts focussed on resistivity measurements near room temperature. Theoretical analyses of the resistivity as a function of dopant density for n-type silicon has been reported by Rode[3] and Norton *et al.*[2]; their calculations of resistivity were also confined to room temperature. In this work, we have extended the theoretical calculations of resistivity as a function of dopant density for n-type silicon to $10^{13} < N_D < 10^{19}\,cm^{-3}$, and $100 < T < 500$ K.

The resistivity is calculated from the expression

$$\rho = \frac{1}{qn\mu_n} \tag{23}$$

If both ρ and n are measured independently, then the electron mobility may be deduced from eqn (23). On the other hand, if μ_n and n are computed from the theoretical expressions discussed above, it is then possible to compare between theoretically computed and experimentally measured resistivity.

Figure 5 shows the resistivity versus donor density for n-type silicon at 300 K; the solid line is our theoretical calculation, and the dashed line is the Irvin curve[23]. The calculated resistivity is 5 to 10% smaller than the resistivity curve given by Irvin[23], which is consistent with recently published resistivity data[24, 29].

In order to compare theory with experiment for temperatures other than 300 K, resistivity measurements were made between 100 and 500 K on seven phosphorus-doped silicon wafers with densities from 1.2×10^{14} to $2.5 \times 10^{18}\,cm^{-3}$.

The resistivity measurements were performed using a planar four-probe test structure[27]. This test structure was designed for bulk resistivity measurements and was fabricated using a bipolar transistor process. The test cells used for resistivity measurements were obtained from the same silicon wafers fabricated for the mobility measurements at 300 K (see Fig. 1). For temperature dependent measurements, the test cell containing the four-probe structure was mounted on a TO-5 header, and a temperature-sensing diode was also mounted next to the cell for measuring the temperature. The TO-5 header was then mounted inside a specially-designed cryostat where temperatures can be varied from −191 to 400°C with a maximum heating rate of 7°C/s[31].

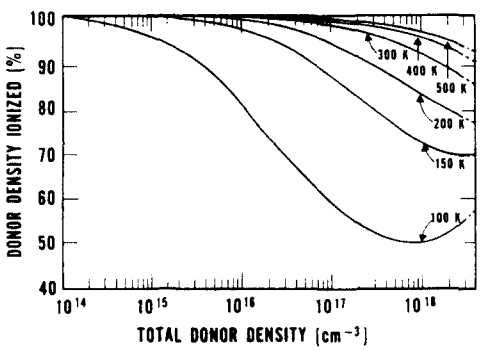

Fig. 4. Percent of ionized phosphorus impurity density vs total phosphorus density with temperature as a parameter ($100 < T < 500$ K).

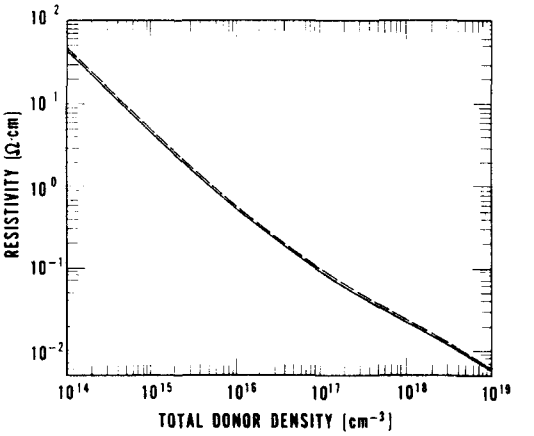

Fig. 5. Resistivity vs total donor density for n-type silicon at 300 K. Solid line is the theoretical calculation and the dashed line is from the Irvin curve[23].

Figure 6 shows the plot of resistivity as a function of temperature for phosphorus-doped silicon with dopant densities from 1.1×10^{15} to 2.5×10^{18} cm^{-3}; the solid lines are the theoretical calculations and the solid dots are the measured resistivity. Figure 7 displays the calculated resistivity vs temperature for dopant densities from 5×10^{13} to 10^{19} cm^{-3} in more regular steps. Figure 8 shows the calculated resistivity curves as a function of dopant density for temperatures between 100 and 500 K. The results show that the resistivity depends strongly on temperature for $N_D < 10^{16}$ cm^{-3} where lattice scattering is dominant. However, the resistivity is less dependent on temperature for $N_D > 10^{18}$ cm^{-3} where mixed-scattering prevails.

4. CONCLUSIONS

An improved theoretical model for computing electron mobility as functions of dopant density and temperature in n-type silicon has been formulated. In addition to considering the contributions from scattering by lattice phonons, ionized impurities, and neutral impurities, this model takes into account the effect of electron–electron scattering on both lattice and ionized impurity scattering mobilities for dopant densities greater than 2×10^{16} cm^{-3}. From the present study, it was found that the influence of e–e scattering is negligible for $N_D \leq 2 \times 10^{16}$ cm^{-3}, but is significant for $N_D \geq 2 \times 10^{17}$ cm^{-3}. To allow a smooth change in mobility across the boundaries of the transition region (i.e. $2 \times 10^{16} \leq N_D \leq 2 \times 10^{17}$ cm^{-3}), the effect of e–e scattering is assumed to increase linearly with the dopant density in this region. The theoretical calculations, based on such model, are with ±5% of the measured mobility for $10^{13} \leq N_D \leq 10^{19}$ cm^{-3} and $T = 300$ K.

Resistivity analysis for phosphorus-doped silicon shows that for dopant densities less than 3×10^{18} cm^{-3}, the theoretically predicted resistivity values are within ±7% of the experimental data for temperatures between 100 and 500 K.

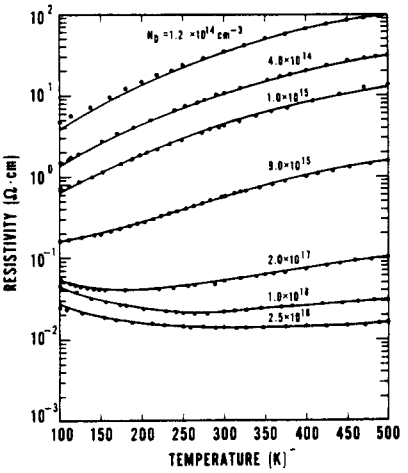

Fig. 6. Resistivity vs temperature for seven phosphorus-doped silicon samples. Solid lines are the theoretical calculation and dots are the experimental data.

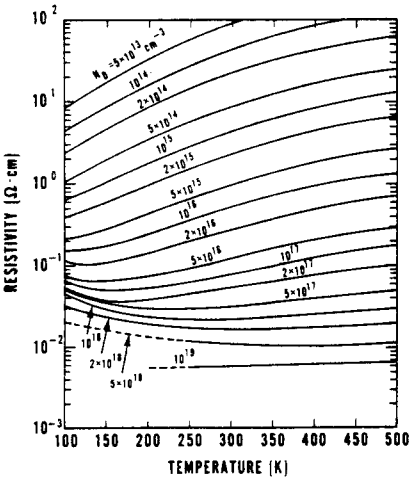

Fig. 7. Theoretical calculations of resistivity vs temperature for n-type silicon for dopant densities from 5×10^{13} to 10^{19} cm^{-3}.

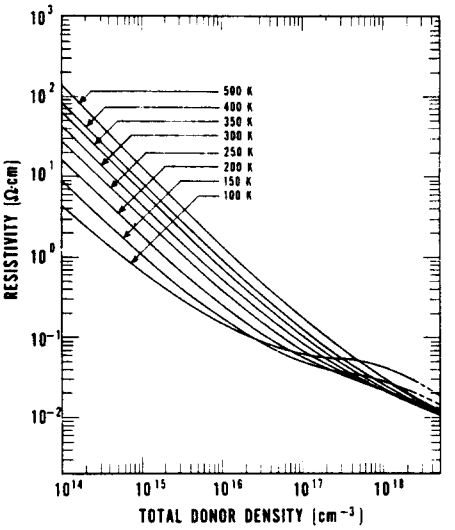

Fig. 8. Theoretical calculations of resistivity vs total donor density for n-type silicon with temperature as a parameter ($100 < T < 500$ K).

Acknowledgements—The authors would like to thank Drs. W. M. Bullis and M. G. Buehler for their critical review of the manuscript and their encouragement during the course of this study. One of the authors (Li) would like to thank Dr. W. E. Phillips for his assistance in using the cryogenic system for resistivity measurements. He is also grateful to the technical staff of the Electronic Technology Division for their cooperation.

REFERENCES

1. D. Long, *Phys. Rev.* **120**, 2024 (1960).
2. P. Norton, T. Braggins and H. Levinstein, *Phys. Rev. B* **8**, 5632 (1973).
3. D. L. Rode, *Phys. Status Solidi (b)* **53**, 245 (1972).
4. C. Herring and E. Vogt, *Phys. Rev.* **101**, 944 (1956).
5. H. Brooks, *Theory of the Electrical Properties of Germanium and Silicon, Advances in Electronics and Electron Physics* (Edited by L. Marton), Vol. 7, pp. 85–182. Academic Press, New York (1955).
6. C. Herring, *Bell Syst. Tech. J.* **36**, 237 (1955).
7. R. B. Dingle, *Phil. Mag.* **46**, 831 (1955).
8. A. G. Samoilovich, I. Ya. Korenblit, I. V. Dakhovskii and V. D. Iskra, *Sov. Phys.-Solid State* **3**, 2385 (1962).
9. D. Long and J. Myers, *Phys. Rev.* **115**, 1107 (1959).
10. D. Long, *Phys. Rev.* **129**, 2464 (1963).
11. C. Erginsoy, *Phys. Rev.* **79**, 1013 (1950).

12. N. Sclar, *Phys. Rev.* **104**, 1559 (1956).
13. M. Luong and A. W. Shaw, *Phys. Rev. B* **4**, 2436 (1971).
14. L. Spitzer, Jr. and R. Härm, *Phys. Rev.* **89**, 977 (1953).
15. P. P. Debye and E. M. Conwell, *Phys. Rev.* **93**, 693–706 (1954).
16. F. J. Blatt, *Solid State Physics* (Edited by F. Seitz and D. Turnbull), Vol. 4, p. 356. Academic Press, New York (1957).
17. J. S. Blakemore, *Semiconductor Statistics*, p. 360. Pergamon Press, London (1960).
18. H. D. Barber, *Solid-St. Electron.* **10**, 1039 (1967).
19. G. L. Pearson and J. Bardeen, *Phys. Rev.* **75**, 865 (1949).
20. N. A. Penin, B. G. Zhurkin and B. A. Volkov, *Sov. Phys.-Solid State* **7**, 2580 (1966).
21. F. J. Morin and J. P. Maita, *Phys. Rev.* **96**, 28 (1954).
22. S. M. Sze and J. C. Irvin, *Solid-St. Electron.* **11**, 599 (1968).
23. J. C. Irvin, *Bell Syst. Tech. J.* **16**, 387 (1962).
24. F. Mousty, P. Ostoja and L. Passari, *J. Appl. Phys.* **45**, 4576 (1974).
25. W. M. Bullis, F. H. Brewer, C. D. Kolstad and L. J. Swartzendruber, *Solid-St. Electron.* **11**, 639 (1968).
26. P. W. Chapman, O. N. Tufte, J. D. Zook and D. Long, *J. Appl. Phys.* **34**, 329 (1963).
27. M. G. Buehler, *Semiconductor Measurement Technology.* NBS Spec. Publ. 400-22 (1976); M. G. Buehler and W. R. Thurber, *IEEE Trans. Electron Dev.* **ED-23**, 968 (1976).
28. G. Baccarani and P. Ostoja, *Solid-St. Electron.* **18**, 579 (1975).
29. R. L. Mattis and M. G. Buehler, *Semiconductor Measurement Technology.* NBS Spec. Publ. 400-11 (June 1975).
30. D. M. Caughey and R. E. Thomas, *Proc. IEEE* **55**, 2192 (1967).
31. M. G. Buehler and L. M. Smith, *Thermally Stimulated Properties* (Edited by W. M. Bullis) NBS Tech. Note 788, pp. 12–14 (August 1973).
32. S. S. Li, *Semiconductor Measurement Technology.* NBS Special Publication 400-33, March (1977).